

FAST REGISTRATION-BASED AUTOMATIC SEGMENTATION OF SERIAL SECTION IMAGES FOR HIGH-RESOLUTION 3-D PLANT SEED MODELING

F. Bollenbeck and U. Seiffert

Leibniz Institute of Plant Genetics and Crop Plant Research, Pattern Recognition Group
06466 Gatersleben, Germany

ABSTRACT

We propose a deformation-based approach for fast and robust segmentation of histological section images into multiple tissues. Derived from deformable registration techniques, it does not solely rely on information present in the image, but uses *a-priori* information in terms of reference segmentations.

The experimental evaluation against state-of-the-art feature based classifiers demonstrates the high performance in segmentation accuracy and the effectiveness of this approach. This serves as basis for processing high-resolution serial section datasets comprising several thousand images towards three-dimensional atlases of plant organs.

Index Terms— Image segmentation, Image registration, Modeling, Biomedical microscopy

1. INTRODUCTION

Digital models of biological objects have proven to deliver new facilities for the analysis of structural and functional interrelationships as well as developmental processes in a spatial or spatio-temporal context [1][2][3].

We are working towards the generation of a generalized 3-D anatomical atlas of developing barley (*Hordeum vulgare*) grains at different developmental stages. Serving as reference framework for the integration, visualization, and exploration of various data modalities, such inter-individual atlases significantly promote the analysis of developmental gradients and dynamics.

Considering different time points and individuals, models are constructed on the basis of tens of thousands serial section images composing gigabytes of image data, drastically reducing the allowed computational complexity in the model-generation pipeline.

The gain in resolution and histological detail with serial section data comes with additional expenses in processing, since the object of interest is essentially physically destroyed for digitization. This necessitates a fast and robust method for the expert-based segmentation of serial section data, aside from the use of well tuned and adapted algorithms for reconstruction.

This work is supported by the BMBF grant 0312821. The authors want to thank U. Siebert and B. Zeike for the material preparation, T. Czuderna, A. Ihlow, R. Pielot, and W. Weschke for fruitful discussions and useful comments.

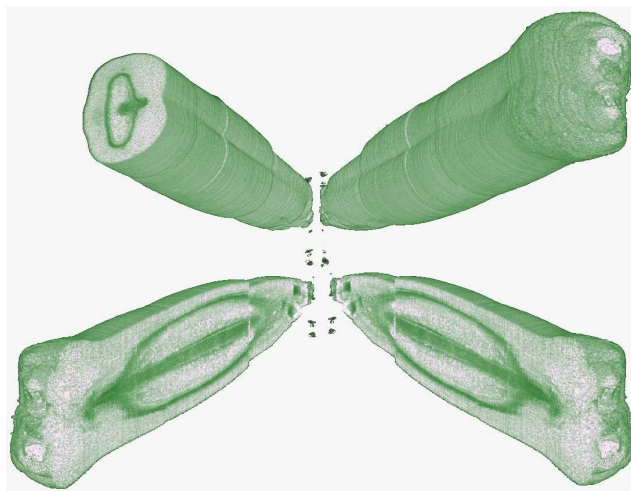


Fig. 1. Perspectives of a digital barley grain. A volume rendering of standardized and registered stack of serial section images. The reconstruction procedure yields an intact grain histology, enabling virtual sections in any desired direction. The dataset is approximately 4 GB.

2. IMAGE ACQUISITION AND PREPROCESSING

The imaging of functional units and tissues in sectioned plant material on a micrometer scale using light microscopy requires preparation including the treatment with a contrasting agent. Plant material is cut into $3\ \mu\text{m}$ thick slices with a microtome and subsequently digitized with a light microscope at a spatial resolution of $1,83 \times 1,83\ \mu\text{m}$ per pixel¹, composing a dataset of roughly 2,000 images per grain.

To account for disturbances in the images the region-of-interest (*ROI*) must be masked against the image background since particles occur on the microscope slides, mostly being high-frequency noise, using edge-detection and blob-analysis.

Arbitrary positioning and orientation of the grain objects on the microscope slide are standardized employing the well-established *Principal Axis Transform (PAT)*, also yielding a bulk-transform initialization for the subsequent stack registration.

¹Colorspace analysis shows almost linear correlation for the contrasting, therefore the images were digitized as grayscale-intensities with minimal loss.

The full image stack is rigidly registered to reconstruct the sectioned object by finding an optimal superposition of all images in the stack. We use a spatially extended image-to-image metric of a weighted sum of *SSD* metric² values within a local neighborhood of slices for more robust stack registration. The registration also includes re-sampling to isotropic voxel-sizes. Figure 1 shows a volume rendering of a reconstructed intensity dataset.

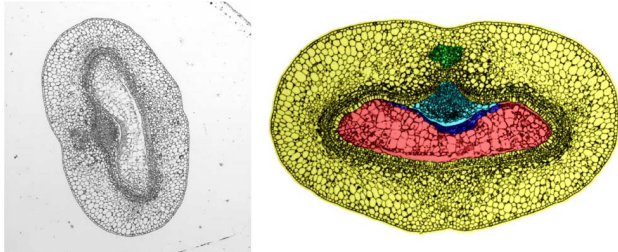


Fig. 2. Figure showing a raw-image cut-out with minor disturbances and the standardized equivalent in uniform background. Colored regions show the segmentation into present tissues.

3. SEGMENTATION OF SECTION IMAGES

Segmentation often is the crucial step where expert knowledge is needed, since here the raw-data is abstracted towards the purpose of the modelling. Labeled voxel-data is the basis for quantification and surface-based modelling of internal structures.

In the segmentation step relevant biological structures within an image $I : \Omega \subset \mathbb{R}^2 \mapsto \mathbb{R}^+$ are recognized and assigned a unique label $S : I \subset \Omega \mapsto \{1, \dots, M\}$ for M tissues or classes.

An automatic segmentation of sections is characterized by several requirements:

- A multitude of tissues must be recognized
- Images lack clearly defined edges and structures
- The identification of tissue types needs expert knowledge

which necessitates the use of algorithms incorporating *a priori* information for robust multiclass-segmentation, where solely intensity-based techniques are clearly unfeasible.

One possible encoding of *a priori* information (e.g. class numbers and densities) are manual reference segmentations of sample images, thereby facilitating segmentation algorithms resembling expert knowledge autonomously without human interaction or control being necessary.

3.1. Reference-based Image Segmentation

We solve the segmentation task via a registration problem, exploiting a consequence of the sectioning: Although the

²Here the computational cheap *Sum Of Squared Differences (SSD)* is used, because of intensity equalization in the preprocessing steps.

segmentation of an individual image is tough, neighbouring images are similar in their respective tissue mapping.

Atlas-based registration and deformation for example has been suggested for segmentation of brain MR-data [4][5]. Where these approaches are based on a fully segmented volume as reference, using either *optical flow* equations [4] or *level-sets* [5] to segment a new instance, a full (manual) reference segmentation of a gigavoxel sized serial section dataset is clearly impractical.

An optimal rigid alignment of the stack images given, a reference segmentation is adapted based on the similarity of the reference image slice to the target image slices using a registration approach.

For section images $R, T : \Omega \subset \mathbb{R}^2 \mapsto \mathbb{N}^+$ with a reference segmentation $S : R \subset \Omega \mapsto \{1, \dots, M\}$ of R a transformation of S to segment R correctly is found by an optimal deformation of R to T . Given the reference intensity image R and template intensity image T the goal is to find a transformation to maximize the similarity between both images. The transformation u is now non-parametric or *free-form* in contrast to the affine transformation for the stack registration, allowing arbitrary pixel displacements.

The problem of finding an optimal deformation u maximizing an image-to-image metric D needs to be regularized, leading to the well-known *deformable* registration problem [6][7]

$$\mathbf{J}(u) := D(R, T; u) + \alpha s(u) \stackrel{!}{=} \min .$$

For the regularizer or smoothing term s we elide the physically motivated *elastic* potential introduced by [7] in favour of a gradient-based diffusion regularizer [8][9]. While delivering explicitly smooth displacement fields, the diffusion-registration problem can be solved in $\mathcal{O}(N)$ per registration step using state-of-the-art solution schemes as in [9], on which we rely.

As a result of the registration procedure we do not employ the registered (transformed) template image, but the transformation u in form of a displacement field, which is applied to transform S to obtain a segmentation of the target image T . Subsequently, the adapted segmentation is mapped back to the original label interval by direct binning, since labellings on interpolation gridpoints outside the label set $\{1, \dots, M\}$ occur.

3.2. Supervised Classification Segmentation

Image segmentation based on a pixel-wise classification in a supervised classification scheme has been proposed for high-accuracy results on various image data, including histological sections of biological specimen [10]. We used two supervised classification schemes based on local features for benchmarking the reference-based segmentation approach.

3.2.1. Local Features

In order to compile a discriminant feature vector for the classification, we extracted a set of standard-features for each pixel in the grayscale images. For the textured nature of section images, features are based on spatial variations in the gray-value distributions of local pixel neighborhoods. Texture is known as a powerful feature for image classification

Method \ Class (class density)	1 (42.18%)	2 (40.64%)	3 (1.21%)	4 (4.37%)	5 (1.22%)	6 (10.42%)	Total ACC	rel. Comp. Time
Deformation Based	0.9931 ± 0.0078	0.9925 ± 0.0049	0.8281 ± 0.03137	0.9643 ± 0.0178	0.7269 ± 0.02426	0.9118 ± 0.0959	0.9782 ± 0.0303	1.0
one-vs-rest RBF SVM	0.8927 ± 0.0035	0.8913 ± 0.0018	0.1643 ± 0.3433	0.8531 ± 0.1325	0.4204 ± 0.1899	0.8366 ± 0.0253	0.8703 ± 0.1161	15.6
30-15-logsig MLP	0.8854 ± 0.0086	0.8091 ± 0.0271	0.1701 ± 0.3087	0.7957 ± 0.3119	0.1539 ± 0.2899	0.7763 ± 0.2624	0.8218 ± 0.2014	12.1

Table 1. Assessment of the segmentation algorithms on the reference dataset: Examination of the segmentation accuracy for each tissue class, displaying the per-pixel true positive rates w.r.t. to the reference segmentation (see Section 4.1). The deformation-based method clearly outperforms both supervised classifiers. SVM and MLP are especially less sensitive for classes with a lower overall density (class distribution given in percent). The overall accuracy accordingly aggregates best for the deformable segmentation. The last column indicates the higher computational demands of the supervised approaches in terms of a normalized computation time (average per image, including feature extraction, training, and classification).

and segmentation in the literature, and we therefore adapted several approaches for multitexture feature extraction:

- A set of *Gabor*-filters with different scales and angles
- *Gray-Level Cooccurrence Matrices* for different spatial relations and derived statistics
- *Discrete Wavelet Packet Frame* decomposition
- *Range, Entropy, StdDev*, within different local neighborhoods

Optimal parameters were estimated via spectral analysis, guaranteeing high discriminative power for the feature set, non-informative features were identified via *Linear Discriminant Analysis* and rejected.

3.2.2. SVM and Neural Network Segmentation

Generally the connectionist paradigm of *Artificial Neural Networks (ANN)*[11] as well as the *large-margin Support-Vector-Machines (SVM)*[12] have proven to deliver powerful classification tools in various applications including image classification and segmentation. We use *Feed-Forward Networks (MLP)* and a *one-vs-rest SVM* for the classification of pixel-feature data. The reader may be referred to the literature for details.

4. RESULTS

4.1. Assessment of the Segmentation Accuracy in a Supervised Test Scenario

The correct functioning of reprocessing and stack reconstruction was proven on the full section data of five individual barley grains (see figure 1). To demonstrate the accuracy and robustness of the deformation-based segmentation algorithm in particular we followed a two step procedure: In a preliminary experiment we used a sub-stack of 80 images manually labeled by a biologist as a reference to benchmark the accuracy of the deformation-based segmentation against the pixel-based segmentation with MLP and SVM on the extracted features.

10% equidistant stack images were used as reference segmentation for the deformation segmentation algorithm. SVM

and feed-forward net were trained with 10 train-test cycles on equally distributed samples picked at random, employing a 30 – 15 *logsig* hidden-layer net architecture, and one-vs-rest RBF kernel SVMs.

Table 1 shows that the classwise segmentation accuracy of the deformation-based segmentation is significantly better than the supervised classification, with the overall accuracy greater than **97%**.

4.2. Application of the Algorithm in Large-scale Model Generation

We used the deformation-based segmentation creating three-dimensional histological models of individual barley grains. Working towards a statistically valid atlas of barley grain development, serial section images of five individual barley grains were acquired. Due to individual variances in grain growth, each grain was sectioned to 2, 128 to 2, 736 slice images, each of size 1200 × 1600 pixels, adding up to a total data volume of 30 GB.

After preprocessing and stack registration, the dataset was partitioned into sub-stacks. In each substack less than 5% of equidistant spaced slice images were manually segmented by a biologist to further enforce a minimal overhead for expert data using the proposed method. These served as references in the processing of the full dataset, yielding a three-dimensional histological atlas of five developing barley grains.

For visual inspection of differentially labeled areas, we employed an extension of the standard marching cubes algorithm implemented in the *AMIRA* software suite for its capability of extracting surfaces from multiple iso-volumes. Figure 3 shows a surface rendering of one of five grain models which were constructed.

As expected from the preliminary tests, the fitness-of-use of the segmentation algorithm was confirmed on large datasets. Biologically correct segmentations of whole barley grains could thereby be generated, also proving the preprocessing and reconstruction steps (see Figure 1).

5. DISCUSSION

We presented a work-flow of interleaved steps for the construction of 3-D histological atlases based on high-resolution serial sections, utilizing a novel method for the segmentation of serial section data. Addressing the segmentation task via an image-to-image registration problem turned out to be suitable for the expert-based labelling of complex histological section images, and clearly outperformed state-of-the-art supervised segmentation techniques resembling expert knowledge. Both the test case as well as the large scale application proved the high accuracy and usability of the deformation-based segmentation algorithm. The drastically reduced computational overhead of this method in comparison to feature-based segmentation (Table 1) is a prerequisite for the generation of high-resolution histological models. High-throughput modeling is particularly essential to quantify and incorporate individual variances from multitudes of specimen and thereby constructing statistically valid averaging-atlases. Since the underlying paradigm of deformable image registration is not limited to section images, a generalization application towards other image modalities and sources is feasible.

In a biological context, volumetrics of the individual volume datasets delivered new insights into the variances of the composition of different tissues within barley grains. Further, 3-D models serve as spatial framework for the integration of other data sources, a reference map for tissue specific microdissection assays, and as a visualization aid for analysis. A robust and fast model-generation pipeline is the basis for an individual-averaging atlas which will be resolved on a timeline (4D models), promoting the systematic analysis of developing barley grains.

6. REFERENCES

- [1] M. Ringwald, R.A. Baldock, J. Bard, M.H. Kaufman, J.T. Eppig, J.E. Richardson, J.H. Nadeau, and D. Davidson, "A Database for Mouse Development," *Science*, vol. 265, pp. 2033–2034, 1994.
- [2] K. Rein, M. Zöckler, M. T. Mader, C. Grubeland, and M. Heisenberg, "The Drosophila Standard Brain," *Current Biology*, vol. 12, no. 3, pp. 227–231(5), 2002.
- [3] W. Pereanu and V. Hartenstein, "Digital three-dimensional models of Drosophila development," *Cur. Opin. Genet. Dev.*, vol. 14, pp. 382–391, 2004.
- [4] B.M. Dawant, S.L. Hartmann, J.P. Thirion, F. Maes, D. Vandermeulen, and P. Demaerel, "Automatic 3-d Segmentation of Internal Structures of the Head in MR Images using a Combination of Similarity and Free-Form Transformations," *Medical Imaging*, vol. 18, no. 10, pp. 909–916, 1999.
- [5] C. Baillard, P. Hellier, and C. Barillot, "Segmentation of Brain 3D MR Images using Level Sets and Dense Registration," *Medical Image Analysis*, vol. 5, no. 3, pp. 185–194, 2001.
- [6] J. Modersitzki, *Numerical Methods for Image Registration*, Numerical Mathematics and Scientific Computation. Oxford University Press, 2004.
- [7] C. Broit, *Optimal Registration of Deformed Images*, Ph.D. thesis, 1981.
- [8] B. Fischer and J. Modersitzki, "Fast Diffusion Registration," in *Inverse Problems, Image Analysis, and Medical Imaging*, M.Z. Nashed and O. Scherzer, Eds., Contemporary Mathematics 313. AMS, 2002.
- [9] B. Fischer and J. Modersitzki, "FLIRT: A Flexible Image Registration Toolbox," in *Biomedical Image Registration*, Philadelphia, PA, USA, 2003, LNCS, pp. 261–270, Springer, Heidelberg.
- [10] C. Brüß, F. Bollenbeck, F.-M. Schleif, W. Weschke, T. Villmann, and U. Seiffert, "Fuzzy Image Segmentation with Fuzzy Labelled Neural Gas," in *Proc. of the 14th European Symposium on Artificial Neural Networks ESANN*, 2006.
- [11] S. Haykin, *Neural Networks: A Comprehensive Foundation*, Prentice Hall PTR, 1998.
- [12] V. Vapnik, *The Nature of Statistical Learning*, Springer Verlag, New York, 1995.

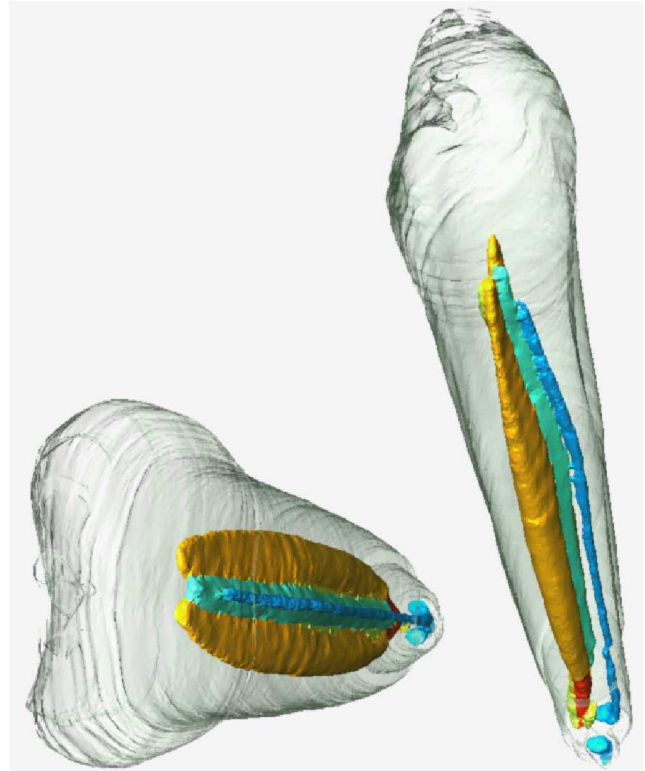


Fig. 3. Two perspectives of an iso-surface rendering of one segmented grain volume constituting of 2280 section images.